

A Pneumatically-Driven Soft Robot Biologically Inspired by Earthworms

Ariel A. Calderón, Juan C. Zagal, and Néstor O. Pérez-Arancibia

Abstract—We present the design, fabrication and feedback control of an earthworm-inspired soft robot capable of locomoting inside pipes. The bodies of natural earthworms are composed of repeated deformable structural units, actuated by axial and longitudinal muscles, employed to generate the body motions required for limbless locomotion, such as burrowing. Following this basic notion, we propose a new pneumatically-driven soft robotic system, built by integrating together two radial actuators with an axial actuator, which mimics the motion and functionality of one body segment of a natural earthworm. The suitability of the proposed approach is demonstrated experimentally through three basic locomotion tests: horizontal motion, vertical motion and oblique motion inside a varying-angle transparent pipe.

I. INTRODUCTION

A distinguishing feature of soft robotic systems is the ability to function in and adapt to inhomogeneous geometrical conditions of the environments in which they operate. For example, [1] presents a highly-flexible pneumatically-driven soft robot capable of walking on unstructured surfaces and performing other tasks difficult to achieve by rigid robots. In this abstract, we describe the development of a soft robotic system designed to replicate some of the characteristics observed in earthworms. Instead of limbs, earthworms employ hydrostatic skeletons to perform the mechanical functions required for locomotion. They extend and contract their muscles to transmit forces to the environment. Hydrostatic skeletons are deformable and their stiffnesses can be varied, traits that can be mimicked by soft robots.

In the case of an earthworm, locomotion is generated by the action of peristaltic waves that pass through the earthworm's body, expanding or relaxing the animal's muscles, and producing axial and radial deformations of the body segments. The speed of locomotion can be described as a function of three variables: stride length (aggregated deformation of the axial muscles per step), protrusion time (time elapsed during the aggregated elongation of the axial muscles) and stance time (time for the peristaltic wave to pass through the earthworm's body) [2]. Pneumatic soft actuators can be programmed to deform according to configurations similar to those of the muscles of earthworms to generate the axial and radial deformations that cause locomotion. In this case, we use feedback control to produce the proper stride lengths, protrusion times and stance times required to effectively mimic the locomotion of natural earthworms.

II. DESIGN, FABRICATION AND CHARACTERIZATION

Earthworms travel underground employing coordinated peristaltic waves of muscular contractions and expansions (relaxations) of their body sections, while some body segments synchronously anchor to the surrounding soil as other body segments detach, as graphically described in Fig. 1-(a) and Fig. 1-(b). In the case of natural earthworms, in order to anchor to the substratum, radially expanded regions of the organisms employ pressure and millimetric claw-like bristles that attach to the surrounding soil. The soft robotic system presented in this extended abstract, shown in Fig. 1-(c), is composed of three body segments (artificial muscles): a rear radial actuator, a central axial actuator and a frontal radial actuator. Notice

This work was supported in part by the Chilean National Office of Scientific and Technological Research (CONICYT) through a graduate fellowship to A. A. Calderón, and in part by the USC Viterbi School of Engineering through a graduate fellowship to A. A. Calderón and a start-up fund to N. O. Pérez-Arancibia.

A. A. Calderón and N. O. Pérez-Arancibia are with the Department of Aerospace and Mechanical Engineering, University of Southern California (USC), Los Angeles, CA 90089-1453, USA (e-mail: aacalder@usc.edu; perezara@usc.edu). J. C. Zagal is with the Department of Mechanical Engineering, University of Chile, Santiago, 8370448, Chile (e-mail: jczagal@ing.uchile.cl).

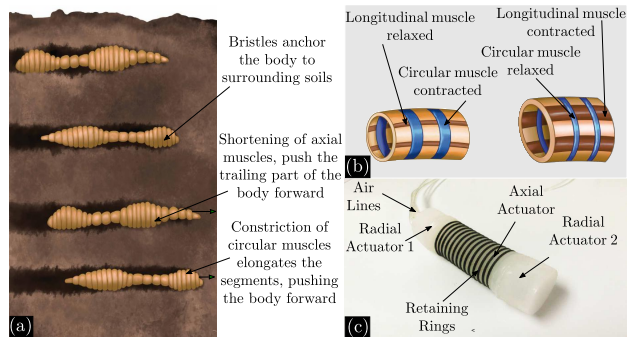


Fig. 1: Natural and artificial worms. (a) Illustration showing the peristalsis-based locomotion of earthworms during burrowing. (b) Illustration showing a segment of an earthworm's body. The blue rings represent circular muscles that contract and relax radially and the brown stripes represent longitudinal muscles that contract and relax linearly, both required to generate body peristaltic waves. (c) Picture showing the biologically-inspired soft robot presented in this abstract. The robot is composed of three actuators: a rear radial actuator, a central axial actuator and a frontal radial actuator. The two radial actuators are the artificial analogues to the circular muscles in blue in Fig. 1-(b) and the axial actuator is the artificial analogue to the longitudinal muscles in brown in Fig. 1-(b).

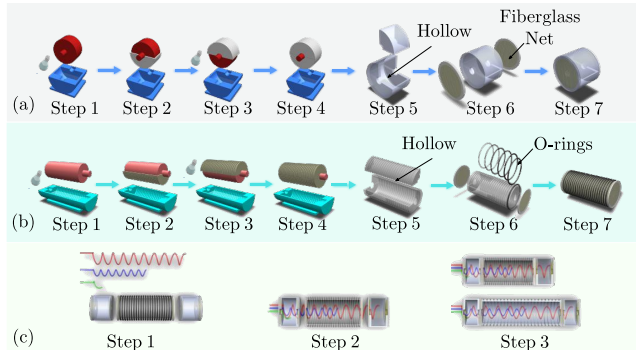


Fig. 2: Fabrication method. The process uses as physical inputs 3-D printed *polylactic acid* (PLA) molds, silicone elastomer (Ecoflex 00-50, Smooth-on), *butadiene* rubber elastomeric o-rings, sheets of fiberglass and pneumatic components. The fabrication process consists of three parts, each consisting of several steps. (a) **Fabrication of a radial actuator:** First, liquid silicone is poured in a mold and the lower half a central plastic body shaft is submerged (Step 1). The mold and silicone are exposed to 60°C for 30 minutes, resulting in a cured semicylindrical hollowed core (Step 2). The core is rotated 180° and the procedure is then repeated to create the second half of the core (Steps 3 and 4). The shaft is removed and a cured silicone cylinder with an internal cavity is obtained (Step 5). The front and rear circular faces of the cylinder are covered with sheets of laminar composite made of soft silicone and a fiberglass net (Step 6). This composite prevents radial deformations of the docking faces while preserving the soft nature of the system axially. Finally, once the lids are cured and sealed, the actuator is finished (Step 7). (b) **Fabrication of an axial actuator:** The same procedure used in the fabrication of a radial actuator in 7 steps. In this case, the mold contains imprinted grooves to lock up *butadiene* o-rings in position during Step 6. (c) **Final assembly:** Two radial actuators, an axial actuator and three helix shaped air feeding lines are integrated into a single functional body.

that this system can be thought of as an artificial version of the body segment between blue rings illustrated in Fig. 1-(b). Therefore, in principle, this is a modular device that can be employed to create artificial worms composed of redundant structures. This inherent modularity brings the potential for the creation of systems that are robust against subsystem failures, less prone to accidents, capable of operating in a wide variety of environments and employing a multiplicity of locomotion modes. The fabrication method and construction sequence used in the manufacture of the soft robot are graphically described in Fig. 2. Here, Fig. 2-(a) and Fig. 2-(b) illustrate the casting processes employed to fabricate the radial and axial actuators, respectively. Additionally, Fig. 2-(c) shows the final procedure used to assemble the subcomponents of the robotic system.

In order to devise a control strategy for locomotion, the robot's actuators are characterized through individual tests in which the internal air pressures are sequentially increased and then decreased to obtain pressure-strain relationship curves.

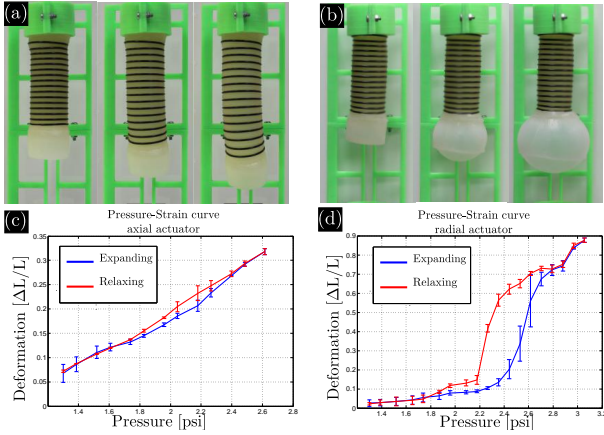


Fig. 3: **Characterization of the actuators.** (a) & (b) Axial actuator and radial actuator during data characterization experiments. (c) & (d) Experimental pressure-strain curves associated with the axial actuator and radial actuator, respectively.

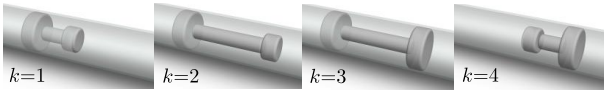


Fig. 4: **Four phases used by the robot to generate one step.** At $k = 1$, the rear radial actuator anchors to the pipe. At $k = 2$, the axial actuator extends to reach a further point. At $k = 3$, the frontal radial actuator anchors to the pipe. At $k=4$, the rear radial actuator and axial actuator relax.

TABLE I: States of the robot's actuators during each phase k .

k	1	2	3	4
Rear Radial Actuator ($i=1$)	1	1	1	0
Axial Actuator ($i=2$)	0	1	1	0
Frontal Radial Actuator ($i=3$)	0	0	1	1

For each actuator, the same test is repeated six times. In situ photographic sequences of an axial actuator and a radial actuator are shown in Fig. 3-(a) and Fig. 3-(b), respectively. The resulting pressure-strain curves for these two actuators are shown in Fig. 3-(c) and Fig. 3-(d), respectively. Notice that the radial actuator displays a pronounced hysteresis, while the hysteresis of the axial actuator is almost insignificant.

III. LOCOMOTION PLANNING AND CONTROL

The actuation sequence employed for locomotion is shown in Fig. 4. Four phases are defined to generate one *step* and two states are defined for each actuator as

$$x_i[k] = \begin{cases} 1 & \text{if } p_i \geq p_{ri} \\ 0 & \text{if } p_i < p_{ri} \end{cases}, \quad (1)$$

where $i = 1, 2, 3$ denotes an actuator according to the convention *rear*, *middle* and *frontal*, k denotes the phase, p_i is the measured pressure of the i th actuator and p_{ri} is the threshold pressure to be surpassed by Actuator i . From (1), it follows that the state of Actuator i takes the value 1 when the actuator is expanded and the value 0 when the actuator is relaxed. The states of the three actuators during each phase k of a *step* are shown in Table I. For each actuator i , a pump increases the pressure inside it until p_{ri} is surpassed, triggering the next *step* phase. Proper thresholds p_{ri} are found as part of the characterization process already described, so that the actuators relax and expand according to the desired robot's deformations required for locomotion. The axial expansion of Actuator 2 determines the stride length, the time it takes for Actuator 2 to expand determines the protrusion time and the stance time is given by the time it takes for the three actuators to expand sequentially, according to the strategy in Fig. 4. Clearly, these three variables directly depend on the thresholds p_{ri} and the rates of the airflows used to expand the actuators.

The use of the proposed locomotion method requires the implementation of low-level controllers on the individual actuators. The basic control scheme for each actuator is shown in Fig. 5-(a) and the high-level hardware and control

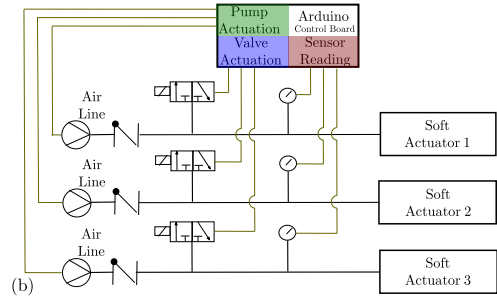
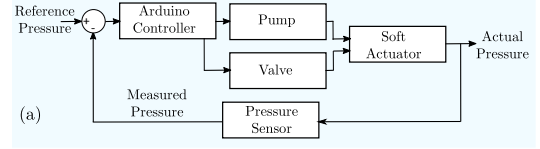


Fig. 5: **Diagrams of the scheme used to control the soft robot during locomotion tests.** (a) Block diagram of the control loop associated with a generic actuator i . (b) Physical connection of the hardware composing the robotic system.

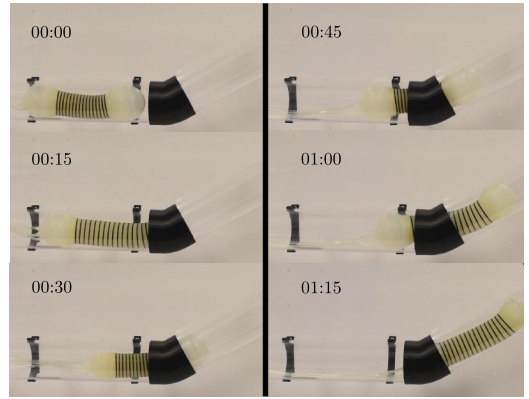


Fig. 6: **Locomotion test.** The robot starts to move horizontally and then autonomously adapts its body to maneuver through a path angle of 45° . The numbers on the upper-left corners show time in minutes:seconds.

scheme of the whole robotic system is shown in Fig. 5-(b). Here, each actuator employs one pump to trigger and sustain actuation. Piezo-resistor-based pressure sensors are employed in the implementation of the low-level control loops shown in Fig. 5-(a) and high-level control algorithm shown in Fig. 5-(b). Solenoid valves are used to vary and regulate the pressures inside the actuators. Thus, when a valve is closed, the corresponding actuator's internal pressure increases, as its pump supplies air continuously. Analogously, when a valve is open, the corresponding actuator relaxes and reaches the atmospheric pressure. All the control algorithms in Fig. 5 are run on an Arduino processor.

IV. EXPERIMENTAL RESULTS

The robot was tested using three locomotion experiments inside a transparent pipe: horizontal motion, vertical motion and variable inclined motion, all using the same controller. These tests demonstrate that the soft nature of the proposed robotic system allows it to adapt to various operating conditions. The photographic sequence in Fig. 6 shows the evolution over time of the robot while traversing a pipe. In this experiment, the robot begins to move horizontally, then it adapts in order to maneuver through an elbow and continues climbing inside the pipe, which changes its inclination from 0° to 45° . A complete series of horizontal, vertical and inclined locomotion experiments can be found at <http://www.uscaml.com/resources/scr2016/RoboticEarthWorm.mp4>.

REFERENCES

- [1] R. F. Shepherd et al. Multigait soft robot. *Proceedings of the National Academy of Sciences*, 108:20400–20403, 2011.
- [2] K.J. Quillin. Kinematic scaling of locomotion by hydrostatic animals: ontogeny of peristaltic crawling by the earthworm *lumbricus terrestris*. *The Journal of experimental biology*, 202:661–74, 1999.